KUSTAANHEIMO-STIEFEL VARIABLES TO HALVE THE COST OF MONTE CARLO PLANETARY PROTECTION COMPLIANCE ANALYSIS

Alessandro Masat[(1)], **Matteo Romano**[(2)], **Camilla Colombo**[(3)]

[(1)] *PhD Candidate, Department of Aerospace Science and Technology, Politecnico di Milano, Via G. La Masa 34, 20156 Milano, Italy, alessandro.masat@polimi.it*

[(2)] *Postdoctoral researcher, Department of Aerospace Science and Technology, Politecnico di Milano, Via G. La Masa 34, 20156 Milano, Italy, matteo1.romano@polimi.it*

[(3)] *Associate Professor, Department of Aerospace Science and Technology, Politecnico di Milano, Via G. La Masa 34, 20156 Milano, Italy, camilla.colombo@polimi.it*

ABSTRACT

Planetary protection in trajectory design aims to assess the impact probability of space mission disposed objects based on their initial uncertain condition, to avoid contaminating other planetary environments. High precision dynamical models and propagation methods are required to reach high confidence levels on small estimated impact probabilities. These requirements have so far confined planetary protection analysis to robust Monte Carlo-based approaches, using the Cartesian formulation of the full force problem.

This work presents the performance improvements brought by the adoption of the Kustaanheimo-Stiefel (KS) formulation of the dynamics. The KS formulation is here combined with adaptive non-dimensionalisation and reference frame switch procedures upon detection of close encounters. The fibration property of the KS space, namely the parametrisable locus of point arising from the mapping to a higher-dimensional phase space, is exploited to minimise the computational time, accelerating the initial phase of the numerical integration.

Impact probability estimation tasks become even more efficient than the single simulation case, since the regularisation of the dynamics removes the mathematical near-singularity characterising these problems. Despite a almost halved computational burden for Monte-Carlo analysis, the achieved precision remains unchanged, setting a new performance benchmark for planetary protection tasks.

1 INTRODUCTION

Planetary protection compliance requirements introduce a set of technical conditions that any space mission phase or task must contribute to fulfil. In order not to contaminate the environment of any visited planet, care must be taken particularly for those objects which cannot be sterilised because of their function, such as upper stages of launchers. For instance, a mission to Mars has all of its lander components sterilised in advance, so that possible traces of life are not introduced from Earth, but the stages of the launchers are not and cannot be. Furthermore, they are disposed in space once the injection of the payload into its route to Mars is completed, which makes their dynamics completely uncontrolled. Planetary protection policies are developed and maintained every few years by COSPAR (Committe On Space Research) [1]. The work of Kminek et al. [2] outlines the requirements that any European Space Agency's (ESA) mission must fulfil. For disposal objects they turn

into a small body-dependent value of accepted impact probability (lower for higher likelihood to find traces of local life in the specific moon or planet), which must be estimated at 95% confidence level and considering the evolution of the uncontrolled trajectory 100 years forward in time.
Starting from the requirements introduced by Kminek et al. [2], the ESA SNAPPshot suite was developed by Colombo et al. [3] to compute the impact probability of a given initial condition and uncertainty. A Monte Carlo simulation is performed in the Cartesian formulation of the full force dynamics, keeping static reference frame and non-dimensionalisation quantities throughout the integration. The impact probability is then determined as the ratio between the number of runs turning into an impact over the total number of generated samples.
The research of Romano et al. [4] proposed a line sampling method for the computation of impact probabilities. It is a Monte Carlo-based approach, which ensures a better estimate especially for small probabilities and is also more efficient, as it requires less total runs than the standard Monte Carlo. Other work from Romano [5] investigated the influence of numerical schemes in the performance and precision of the SNAPPshot [3] approach. An attempt was also made to develop a covariance propagation technique in the Cartesian formulation of the dynamics, motivating the choice of regularised formulation of this work. Even before flyby events, the propagated continuous covariance quickly degrades when a Cartesian dynamics is used because of the strong non-linearity and the Lyapunov instability of the Kepler problem, requiring to split the uncertainty initial distribution repeatedly and cumulatively [5]. The results obtained in [5], together with other functionalities, contributed to the development of the improved version of the SNAPPshot suite [6].
Regularising the dynamics is not necessarily attached to a new set of coordinates per se, in fact the Kustaanheimo-Stiefel (KS) regularisation was born bringing together two concepts: the first, adding a fourth coordinate trying to describe the Kepler problem as a four dimensional harmonic oscillator, originally presented by Kustaanheimo [7], and the introduction of the time transformation of the Sundman type [8], operated later with the contribution of Stiefel [9]. All the later developments over the newly created KS formalism use to refer to the more comprehensive manuscript by Stiefel and Scheifele [10]. Bond proposed a variation of parameters approach that generically accounts for perturbing effects starting from the original four-vector KS formulation [11].
Saha [12] proposed a quaternion approach to the KS transformation more suitable to the analysis of Hamiltonian systems. Based on the work of Saha, Breiter and Langner [13] explored the role of the preferential direction chosen to perform the regularisation, which they generalised to an arbitrary one of the original three-dimensional space. In fact, almost all the analyses already performed in the context of the KS formulation adhere to the original one proposed by Kustaanheimo and Stiefel [9], where they selected the first coordinate x of the three-dimensional space (x, y, z) as the reference direction for the KS transformation, although this was not necessarily required. Using the same notation as Breiter and Langner [13], choosing x as preferential direction the KS tranformation is identified as KS1, whereas for instance the KS3 version is presented by Saha [12] using the direction z. The work of Breiter and Langner [13] did not stop to this generalisation, but provided new insight to the physical meanings of the KS coordinates themselves.
Partially quoting Breiter and Langner [13] and recalling the quaternion description of rotations, in the KS1 version "the normalised KS variables are the Euler-Rodrigues parameters of the rotation turning the x axis into the direction of the Cartesian position vector which generated the KS coordinates". From this sentence, the physical meaning of the fibration property of the transformation [10, 13, 14] also becomes more clear, recalling that such a rotation may happen in an infinite number of ways. Another work by Langner and Breiter [15] explores the properties of the quaternionic KS formulation in Hamiltonian systems, tackling also the rotating frame case. Some other work in a similar direction was done by Roa and Peláez [16], they make use of the Minkowskian geometry

that was originally proposed by Kustaanheimo and Stiefel [7, 9] to handle close approaches and their hyperbolic geometry. Still Roa et al. also worked on the KS formulation [17], showing that the Lyapunov stability does not apply to the whole KS fiber with respect to the physical time. Roa and Kasdin made use of quaternions also developing a new set of nonsingular orbital elements that models the intermediary evolution of the orbital plane [18].
On the application viewpoint, KS coordinates have already been used in a few applications. Hernandez and Akella [19] developed a Lyapunov-based guidance strategy using KS coordinates to target several types of orbit conditions, e.g. specified angular momentum vector, and applied it to the design of low thrust trajectories. Woollands et al. [20] developed a Lambert solver based on KS coordinates and used it to provide a good initial guess to the Picard-Chebyshev numerical integration of the perturbed two-body problem. Sellamuthu and Sharma analysed the J_2, J_3, J_4 terms of Earth's oblateness and the third body luni-solar perturbation when approximated with a Legendre polynomial expansion with KS coordinates [21, 22, 23]. Using the equation they obtained, they then implemented an orbital propagator and studied the effects of such perturbations on resident space objects with high perigee and highly eccentric orbits.
This work shows that the adoption of KS coordinates in the barycentric restricted relativistic N-body problem makes the computational cost of the single simulations, and therefore of the whole planetary protection compliance analysis, to drop without any sacrifice of precision. The sensitivity of the regularised formulation on flyby events is mitigated implementing a dynamic and automatic frame switch to the primary body whenever a close approach is detected, generating new KS coordinates for the permanence within the sphere of influence. Section 2 summarises the KS-1 formulation for a generic perturbed problem, deriving the equations of motion from the original Cartesian formulation obtaining an incomplete Hamiltonian set that handles the barycentric regularised motion with the same numbers of states as the planetocentric one, also introucing the non-dimensionalisation and frame switch procedures. Section 3 presents the numerical performances of the proposed approach in comparison to the standard formulation currently employed in SNAPPshot [6], for the single simulation case. Section 4 shows the improvements obtained with KS coordinates for the Monte Carlo planetary protection analysis of Solar Orbiter's upper stage of launcher, repeating the test case presented in [6].

2 ADAPTIVE KS FORMULATION

2.1 Two-body problem in KS coordinates

The KS formulation rewrites the two body problem as an isotropic, four-dimensional harmonic oscillator. The conservation of the orbital energy is also introduced, leading to a simple linear ordinary differential equation.
The first formulation was proposed indeed by Kustaanheimo and Stiefel [9, 10], and extended the usual Cartesian position vector $\underline{r} = \{r_1, r_2, r_3\}^T$ into 4-vector with null magnitude in the Minkowski space, by adding the length $r = \sqrt{\underline{r} \cdot \underline{r}}$ as fourth coordinate. The bold notation will be used in the following lines for quaternions, with null fourth component if corresponding to Cartesian vectors, e.g. $\mathbf{r} = \{r_1, r_2, r_3, 0\}^T$. In the initial formulation proposed by Kustaanheimo, the physical coordinates are linked to the spinor regularised coordinates $\mathbf{u} = \{u_1, u_2, u_3, u_4\}^T$ through:

$$\begin{aligned} r_1 &= u_1^2 - u_2^2 - u_3^2 + u_4^2 \\ r_2 &= 2\big(u_1 u_2 - u_3 u_4\big) \\ r_3 &= 2\big(u_1 u_3 + u_2 u_4\big) \\ r &= u_1^2 + u_2^2 + u_3^2 + u_4^2 \end{aligned} \tag{1}$$

Introducing $\mathbf{u}^* = \{u_1, u_2, u_3, -u_4\}^T$[14, 24], the original relation can be re-written in quaternion notation to obtain $\mathbf{r} = \{r_1, r_2, r_3, 0\}^T$ as

$$\mathbf{r} = \mathbf{u}\mathbf{u}^* \tag{2}$$

Quaternions can be seen as hyper-complex numbers with a scalar real part and a vector complex part, with the directions (i, j, k) as elementary elements of the complex hyper-space, for instance:

$$\mathbf{u} = u_1 + iu_2 + ju_3 + ku_4 \tag{3}$$

and their product is ruled by the following relations:

$$\begin{aligned} i^2 = j^2 = k^2 = ijk = -1 \\ ij = -ji = k \\ jk = -kj = i \\ ki = -ik = j \end{aligned} \tag{4}$$

Unless differently specified, multiplications are now intended as quaternion multiplications. The inverse mapping to produce the KS quaternion with vanishing k component and taking the Cartesian direction x as reference, can be written as [14]:

$$\mathbf{u} = \frac{\mathbf{r} + |\mathbf{r}|}{\sqrt{2(r_1 + |\mathbf{r}|)}} \tag{5}$$

The other key concept is the introduction of the fictitious time s, linked to the physical time t through a Sundman [8] transformation:

$$\frac{ds}{dt} = \frac{\beta}{r} e^{\int K dt} \tag{6}$$

with β an arbitrary constant coefficient and K an arbitrary function of position, velocity and time. The flexibility in the choice of K was never explored and the simplest $K = 0$ has become the standard choice. Setting $\beta = 1$ and $K = 0$ to operate the time transformation, replacing $\mathbf{r} = \mathbf{u}\mathbf{u}^*$ and its derivatives and exploiting quaternion algebra, the KS transformation converts the Kepler two-body problem

$$\ddot{\mathbf{r}} = -\frac{\mu}{r^3}\mathbf{r} \tag{7}$$

into

$$\mathbf{u}'' = \frac{h}{2}\mathbf{u} \tag{8}$$

where $\ddot{(\cdot)}$ and $(\cdot)''$ stand for second t and s derivatives respectively, and h denotes the two-body orbital energy.

The mapping from the three-dimensional to the four-dimensional space is of the Levi-Civita type [14], whose conformality property poses a constraint when taking the differential of $\mathbf{u}$. The set of the infinite admissible KS coordinates generated by the same Cartesian position is also reduced to a fiber of the KS space, that can be parametrised by an angular variable φ [14]. This is called fibration property of the KS space, and using the quaternion notation for the it can be easily verified that any quaternion $\mathbf{u}_\varphi$ obtained from the quaternion $\mathbf{u}$ with the relation $\mathbf{u}_\varphi = \mathbf{u}e^{k\varphi}$ produces the same cartesian coordinate $\mathbf{r}$, once mapped back in the three dimensional Cartesian space, with k third component of the vector part of the quaternion [14].

The presented formalism holds for the KS1 case fo the KS formulation, with the Cartesian coordinate x taken as primary reference. Saha [12] presented the concept referring to the z coordinate, Breiter and Langner [13] then extended it to an arbitrary direction of the original Cartesian space, thus the expressions of the fibration property would need to be generalised accordingly if other generation directions are considered.

2.2 Generic perturbations and barycentric KS equations of motion

The generic perturbing acceleration $\mathbf{f}$ can be written as a quaternion with vanishing k component too:

$$\mathbf{f} = f_1 + if_2 + jf_3 + k \cdot 0 \tag{9}$$

and is accounted for simply by an additional non-null term on the right hand side of the equations of motion [14]. The following pair of expressions for the correspondent Cartesian and KS perturbed two-body problem is therefore obtained [14]:

$$\begin{aligned} \ddot{\mathbf{r}} &= -\frac{\mu}{r^3}\mathbf{r} + \mathbf{f}(\mathbf{r}, t) \\ \mathbf{u}'' - \frac{h}{2}\mathbf{u} &= \frac{r}{2}\mathbf{f}(\mathbf{r}, t)\overline{\mathbf{u}}^* \end{aligned} \tag{10}$$

with $\overline{\mathbf{u}} = u_1 - iu_2 - ju_3 - ku_4$ the quaternion conjugate, and thus $\overline{\mathbf{u}}^* = u_1 - iu_2 - ju_3 + ku_4$.
Since the physical time t can appear in $\mathbf{f}(\mathbf{r}, t)$ either implicitly or explicitly, it should still be tracked, even though its removal was necessary to reach a simpler form of the equations of motion. The relation $dt/ds = r$ can be used to add the physical time as another state element for numerical integrations. For the unperturbed problem it could be retrieved analytically, since the fictitious time s scales as the eccentric anomaly [10]. Denoting the square of the quaternion magnitude as $|\mathbf{u}|^2 = \mathbf{u}\overline{\mathbf{u}} = u_1^2 + u_2^2 + u_3^2 + u_4^2$, the two-body energy h can either be computed at each time step with

$$h = -\frac{1}{r}\left(\mu - 2|\mathbf{u}'|^2\right) \tag{11}$$

or be added as another state element as well, and its derivatives are defined by the dot product between the quaternion representations:

$$h' = \mathbf{r}' \cdot \mathbf{f}(\mathbf{r}, t), \quad \dot{h} = \dot{\mathbf{r}} \cdot \mathbf{f}(\mathbf{r}, t) \tag{12}$$

Writing explicitly $\mathbf{f}$ for the N-body perturbation, keeping the frame centered on one of the N-bodies brings:

$$\mathbf{u}'' - \frac{h}{2}\mathbf{u} = -\frac{r}{2}\sum_{\substack{n=1 \\ n\neq n_p}}^{N}\left(\frac{\mu_n(\mathbf{r} - \mathbf{r}_n)}{|\mathbf{r} - \mathbf{r}_n|^3} + \frac{\mu_n \mathbf{r}_n}{|\mathbf{r}_n|^3}\right)\overline{\mathbf{u}}^* \tag{13}$$

with n_p identifying the primary body, included in the definition of the two-body energy h, and $\mathbf{r}_n$ the position vector of the body n with respect to the primary.
A few modifications are required for the barycentric case, since the state $\mathbf{r}$ does not identify the position with respect to the primary. Every gravitational contribution must be included in the right hand side terms, writing $\ddot{(\cdot)}$ through $(\cdot)''$ with the Sundman transformation $dt/ds = r$ of Equation (6) allows to write the Cartesian expression of Equation (10) and the total orbital energy accounting for the N-body potentials h_0 as

$$\begin{aligned} r\mathbf{r}'' - r'\mathbf{r}' &= -\sum_{n=1}^{N}\frac{\mu_n(\mathbf{r} - \mathbf{r}_n)}{|\mathbf{r} - \mathbf{r}_n|^3} \\ \frac{1}{2r^2}|\mathbf{r}'|^2 - \sum_{n=1}^{N}\frac{\mu_n}{|\mathbf{r} - \mathbf{r}_n|} &= h_0 \end{aligned} \tag{14}$$

Finally, writing explicitly the KS variables $\mathbf{u}$ and $\mathbf{u}'$ leads to the barycentric equations of motion:

$$\begin{aligned} \mathbf{u}'' &= \frac{|\mathbf{u}'|^2}{r}\mathbf{u} - \frac{r}{2}\sum_{n=1}^{N}\frac{\mu_n(\mathbf{r}-\mathbf{r}_n)}{|\mathbf{r}-\mathbf{r}_n|^3}\overline{\mathbf{u}}^* \\ \frac{2}{r}|\mathbf{u}'|^2 &- \sum_{n=1}^{N}\frac{\mu_n}{|\mathbf{r}-\mathbf{r}_n|} = h_0 \end{aligned} \tag{15}$$

Sections 3 and 4 will present results accounting for relativistic effects as well, based on an in-house implementation [25] of the post-Newtonian Einstein-Ingfeld-Hoffmann equations proposed by Will [26] as presented by Seidelmann [27]. Their inclusion does not add any computational complexity to the problem, since only the dependence of the perturbing force $\mathbf{f}$ on velocity and acceleration of the N bodies is introduced.

2.3 Energy non-dimensionalisation and dynamic frame switch

When numerically simulating any dynamic phenomenon, well posed reference quantities allow the states' magnitude to remain as close as possible to the unity on average over the whole dynamics, which may boost the numerical performances of the simulator as the time steps taken can be the largest. This aspect becomes even more relevant in case of close encounters, which feature a much faster dynamics compared to the interplanetary phase.
The introduction of the regularisation procedure over one of the N bodies inevitably makes the formulation more sensitive to close approaches with the remaining ones. A simple switch of reference frame to the flyby body when entering its sphere of influence suffices to maintain the KS regularisation benefits all the trajectory long, which will be shown in Section 4 to have a relevant impact on the computational performances especially when computing impact probabilities. The procedure can be summarised as:

1. Convert the state at the entrance/exit of the sphere of influence into its Cartesian and dimensional representation.
2. Change the centre of the reference frame by simple vector summation.
3. Convert the state back in the original formulation and make it non-dimensional according to the newly updated reference length, time, velocity and gravitational parameter.

These considerations highlight the need of implementing an adaptive non-dimensionalisation strategy, not sensitive on the primary dynamics, to be updated upon integration initialisation or reference frame switch in case of flyby events. Particularly:

1. Set $\mu_{ref} = \mu_{primary}$, which can be either the main attractor in two-body-like trajectories or the equivalent gravitational parameter of a multi-body system.
2. Compute an equivalent two body energy as $h = -\frac{\mu_{primary}}{r} + \frac{1}{2}v^2$.
3. Set the reference length as the absolute value of a fictitious unperturbed orbit's semi-major axis $l_{ref} = \frac{\mu_{primary}}{2|h|}$.
4. Set the reference time as $t_{ref} = \sqrt{\frac{l_{ref}^3}{\mu_{ref}}}$.

5. Set the reference velocity as $v_{ref} = \frac{l_{ref}}{v_{ref}}$.

Note that for closed two-body orbits non-dimensionalised in the presented way the orbital period becomes equal to 2π. The choice should be constrained to the sole principal attractor for flyby events whose dynamics is primarily two-body, so that the typical time and length scales can be properly identified.
The performances of the non-dimensionalisation technique itself will be assessed against SNAPPshot's current procedure, based on static reference quantities. For interplanetary tasks, SNAPPshot [3] takes the astronomical unit and the year as typical length and time scales, l_{ref} and t_{ref}, thus:

$$\begin{aligned} l_{ref} &= AU \\ t_{ref} &= Year \\ v_{ref} &= \frac{l_{ref}}{t_{ref}} \\ \mu_{ref} &= \frac{l_{ref}^3}{t_{ref}^2} \end{aligned} \tag{16}$$

2.4 KS fiber exploitation for minimum computational time

The degree of freedom left by the arbitrary choice of the angle φ used to define the KS state vector can be exploited to minimise the number of time steps that shall be taken by the numerical integration process. Any numerical scheme with adaptive step size, such as Runge-Kutta ones, take the initial steps based on the smallest magnitude element of the initial state vector [28]. If the magnitude of a state element is null, the minimum step is initially taken, then increased as more information on the dynamics becomes available. In fact, KS variables feature a vanishing element if $\varphi = 0$, nevertheless they can be optimised in average-sense because of the fibration property at least for those problems whose dominant dynamics is two-body. More complex scenarios, such as low energy applications, would still benefit from the presented approach simply considering an optimal initial condition generation.
In Figure 1 1000 different initial KS conditions $\mathbf{x}_\varphi = \{\mathbf{u}_\varphi^T, \mathbf{u}_\varphi'^T\}^T$ have been simulated, starting from evenly spaced values of φ between 0 and 2π that generate $\mathbf{u}_\varphi = \mathbf{u}e^{k\varphi}$ from $\mathbf{u} = u_1 + iu_2 + ju_3 + k \cdot 0$, for a 100 year simulation of the asteroids Apophis and 2010RF$_{12}$. The states $\mathbf{u}'_\varphi$ are obtained from $\mathbf{u}_\varphi$ through the differential relations available in [14]. The computational setup is the same used in the following analysis and will be detailed in Section 3. The plotted analytical function in Figure 1 is defined as is $f(\varphi) = -\log(\min|\mathbf{x}_\varphi|)$, normalised and shifted to be graphically superposed to the numerical results, and is used to predict spikes and minima of the integration time steps for the different values of φ.
As expected and well predicted by $f(\varphi)$, the number of time steps taken increases the smaller the minimum magnitude element of the initial KS state becomes, allowing also to identify the regions with minimised time steps. The small oscillations that can be seen in the simulation results of Figure 1 are due to the chaotic full dynamics being integrated instead of the unperturbed two-body problem, whose magnitude is anyway much smaller than the time step reduction achieved by selecting the optimal φ instead of, for instance, $\varphi = 0$.
The simulations have been performed in the same framework that will be better detailed in Section 3, also the evolution of the error with respect to the ephemerides data for the two asteriods does not change with φ and is always the one presented in Figure 2, thus as expected the choice of φ can be exploited with the sole purpose of performing faster simulations.

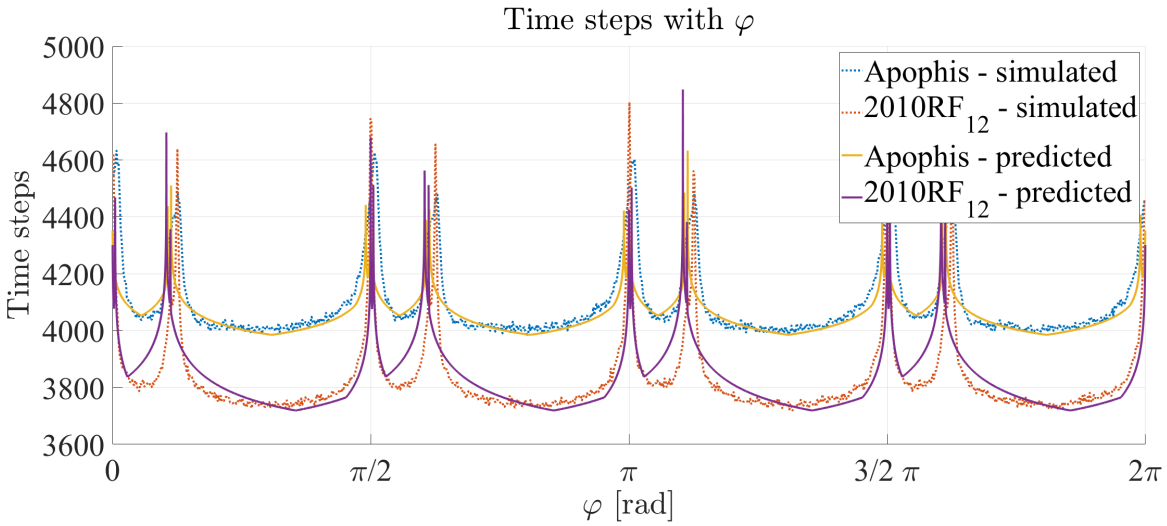

Figure 1: Simulated vs predicted peaks and minima for simulation time steps.

3 SINGLE SIMULATION PERFORMANCES

3.1 Computational setup

The performances of the different simulation strategies in the single long term simulation will be shown for the two near Earth asteroids Apophis and 2010RF$_{12}$, in terms of time steps taken, CPU runtime and error evolution with respect to SPICE data. The initial state was taken from SPICE ephemerides data on the 1st January 1989 at noon and the simulations are carried out 100 years forward in time in the J2000 reference frame. Both the asteroids feature a steep close encounter with Earth within this time span. Due to the prevalent interplanetary nature of the motion the integration neglects J_2 and drag effects. Solar radiation pressure is not considered as the product of the refraction coefficient for asteroids and the area-to-mass ratio is negligible, other than difficult to estimate. The simulations have been performed using an Intel® Xeon® CPU E5-4620 V4 running at 2.10 GHz and using a Runge-Kutta 7/8 integration scheme. All the presented total runtimes are the average of 200 identical runs. Dimensional simulations are not presented, as the maximum number of time steps is reached rather early in the time span. All the presented analyses were performed using Matlab® and interfacing with JPL's ephemerides data through the SPICE toolkit [29] for retrieving the coordinates of the N bodies, considered as all the Solar System's planets plus the Moon.

3.2 Test cases

Figure 2 shows the evolution of the position error of the considered asteroids, identifying the Cartesian integration as Cowell's method. The KS case includes the dynamic frame switch and the adaptive non-dimensionalisation strategy: it was observed that not following this technique introduced numerical instabilities especially at the flyby event, leading to the minimum time step size taken witout reaching the end of the integration span.
It can be seen that the two formulations are equivalent in terms of accuracy, suggesting to choose the less computationally intensive one, since the frame switch and the adaptive reference dimensions make the KS simulation converge. For either case the precision does not change when considering a reference frame centred either the Sun or the Solar System's Barycentre, although the latter was observed to require a lower runtime.

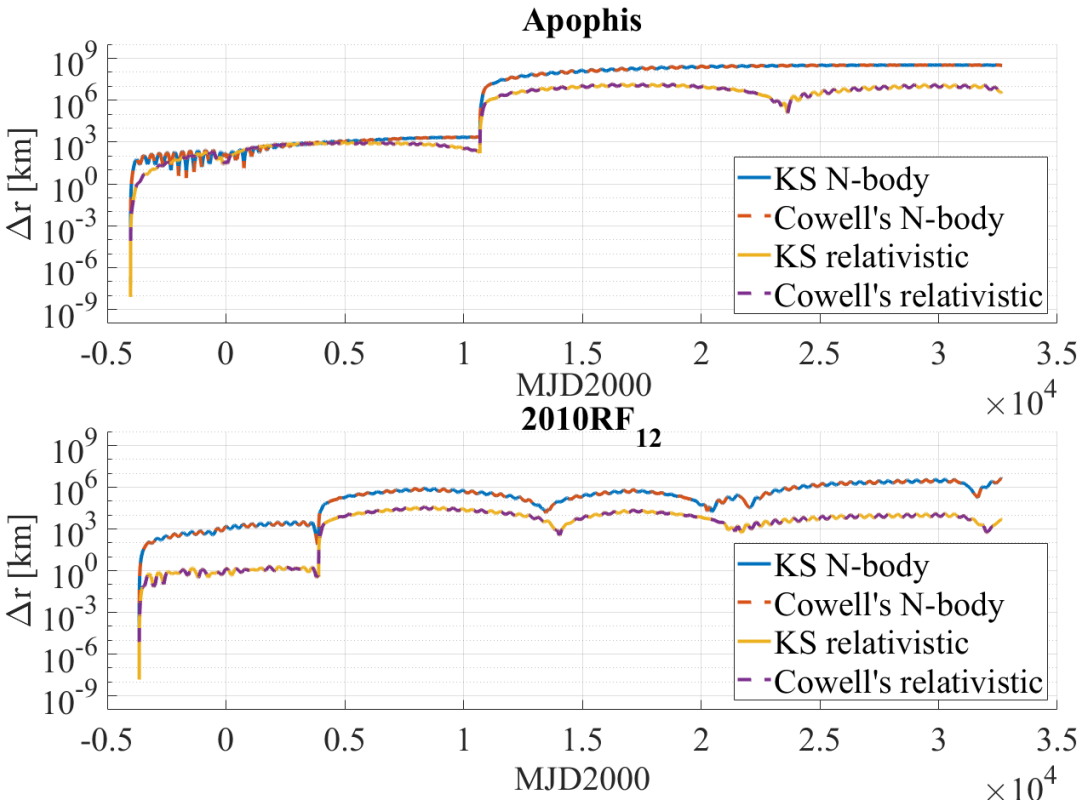

Figure 2: Position error evolution for the different force models and formulations, Apophis and $2010RF_{12}$.

Table 1 compares the runtimes and the number of steps taken by the Cowell's method and the KS formulation, the former featuring SNAPPshot's static non-dimensionalisation, centred on the Sun and without impact or flyby event computation, the latter centred on the Solar System's barycentre and implementing all the presented techniques.
It can be seen in both cases that the integration time steps are reduced by basically 40%, whereas the runtime reduction is slightly lower. This is due to the static integration performed for the benchmark case, whereas the frame switch event is persistently checked in the case of KS integration. For practical applications, for instance the impact computation in planetary protection analyses as it will be shown in Section 4, such events are always considered, leading to the same simulation speed-up obtained theoretically on the total time steps.

4 SOLAR ORBITER'S MONTE CARLO PLANETARY PROTECTION ANALYSIS

The case of the upper stage of the launcher of Solar Orbiter is presented, performing a Monte Carlo simulation with samples generated from the uncertainty on the initial condition given as a covariance matrix, reported in Table 2 and with initial condition given in Equation (17). Such data have been taken from [3], where this test case was studied first. Note that it refers to a mission profile later discarded, whose launch was originally scheduled for late 2018 and ultimately happened in February 2020. The presented results have been obtained with the same simulation routines used for the just discussed single simulation cases.

Table 1: Time steps and runtimes for the Cowell's Sun-centric with static non-dimensionalisation and the KS barycentric adaptive formulations.

CASE	FEATURES		TIME STEPS	TOTAL RUNTIME
Apophis	**Relativity**	No	7357	34.88 s
	Formulation	Cowell's		
	Relativity	No	4025	23.19 s
	Formulation	KS		
	Relativity	Yes	7316	44.24 s
	Formulation	Cowell's		
	Relativity	Yes	4007	26.89 s
	Formulation	KS		
2010RF$_{12}$	**Relativity**	No	6934	33.72 s
	Formulation	Cowell's		
	Relativity	No	3765	21.88 s
	Formulation	KS		
	Relativity	Yes	6929	42.09 s
	Formulation	Cowell's		
	Relativity	Yes	3782	25.34 s
	Formulation	KS		

$$\mathbf{r}_s = \begin{Bmatrix} 132048839.02 \\ 63140185.88 \\ 27571915.38 \end{Bmatrix} \text{ km} \; ; \qquad \mathbf{v}_s = \begin{Bmatrix} -12.20 \\ 20.24 \\ 9.77 \end{Bmatrix} \text{ km/s} \tag{17}$$
$$t_0 = 6868.62 \text{ MJD2000 (midnight)}$$

Table 2: Covariance matrix associated to the initial state of the launcher of SolO at the epoch 6868.62 MJD2000 expressed in the J2000 reference frame [3].

i [km]	j [km]	k [km]	v_i [km/s]	v_j [km/s]	v_k [km/s]
$5.35139E+04$	$5.40992E+04$	$-2.56206E+04$	$2.48201E-01$	$2.74411E-01$	$-1.20515E-01$
$5.40922E+04$	$1.35541E+05$	$4.50788E+03$	$2.33655E-01$	$7.10015E-01$	$3.42692E-02$
$-2.56206E+04$	$4.50788E+03$	$1.72826E+05$	$-1.37013E-01$	$5.01510E-02$	$8.33312E-01$
$2.48201E-01$	$2.33655E-01$	$-1.37013E-01$	$1.15577E-06$	$1.17908E-06$	$-6.48488E-07$
$2.74411E-01$	$7.10015E-01$	$5.01510E-02$	$1.17908E-06$	$3.72423E-06$	$3.07751E-07$
$-1.20515E-01$	$3.42692E-02$	$8.33312E-01$	$-6.48488E-07$	$3.07751E-07$	$4.01929E-06$

A total of 54114 samples has been generated for each case and simulated, based on the results of Wilson's expression [30] as done by Jehn [31] and Wallace [32], and following the implementation proposed in [3].

After the completion of the Monte Carlo simulation, the impact probability of the disposal upper stage of launcher with Earth, Mars and Venus is computed by taking the ratio of the number of simulated impacts over all the generated samples. Table 3 presents the results of two Monte Carlo simulations, parallelising the simulations over 40 cores of the same kind of the one used for the single trajectory simulation. Both cases are propagated in the J2000 reference frame centred on the Solar System's barycentre. Particularly, the Cowell's case persistently checks whether an impact with Venus, Earth and Mars has happened or not at each time step. The KS case switches the integration centre on every

flyby and uses the adaptive non-dimensionalisation strategy. Impacts are searched for only if entering any sphere of influence. Also the same numerical scheme, Runge-Kutta 7/8, is used in both cases and for all the samples.

Table 3: Monte Carlo simulation and related planetary protection analysis showing the impact probability of Solar Orbiter's upper stage of launcher [3], including the time steps taken by and the outcome of the uncertainty barycentre.

CASE	BARYCENTRE		IMPACT PROBABILITY	TOTAL RUNTIME
	RESULT	TIME STEPS		
Cowell's	Impact	1872	4.0211 %	26.66 hours
KS	Impact	88	4.0192 %	14.23 hours

It can be seen that in the Monte Carlo case the simulation speed-up is higher than the single propagation of the asteroids Apophis and 2010RF$_{12}$, achieving a reduction of almost half of the benchmark total runtime. As the number of time steps taken by the barycenter of the generated cloud tell, this is due to the regularised dynamics itself, which can handle the close approaches with much larger time steps than what Cowell's method does. This, in turn, provides the observed performance enhancement: estimating impact probabilities requires analysing what happens close to that celestial body, which is also the main advantage of the KS formulation, as it embeds an adaptive scaling of the physical time for different distances from the primary attractor. This information is more meaningful than the total runtime itself to assess the actual improvements brought by the proposed formulation, since it is not sensitive on possible temporary runtime slow-downs of the computational architecture. Note finally that the estimated impact probability remains basically unchanged, the slight difference might be due to both few borderline cases where the time step that would actually be within the impact region is skipped by the KS integration, and also because of the slightly different samples generated from the initial same covariance matrix (Table 2).

5 CONCLUSION AND OUTLOOK

This work aimed to improve the efficiency of the single simulation strategies, which once performed within a Monte Carlo simulation and post-processed accordingly build a complete planetary protection analysis.

As dimensional propagations are not efficient in general, the adaptive non-dimensionalisation has been shown to also improve the usual simulation techniques using Cartesian coordinates. For the transition to KS coordinates, this choice of reference quantities becomes necessary, as well as switching the center of reference frame becomes mandatory for the simulation convergence.

The primary-centric KS formulation has been implemented and used in the full force problem and its barycentric counterpart has been derived. In general, the KS approach improves the efficiency of numerical simulations as larger time steps can be taken without any precision loss, as the integrated dynamics is always almost linear. Despite the on-paper lost linearity property, the barycentric KS formulation exhibits the best performances overall, both in terms of time steps taken and total runtime required.

The proposed KS formulation has been finally adopted to perform the planetary protection analysis of Solar Orbiter's upper stage of launcher. An even larger relative reduction of the total runtime is obtained, with respect to the presented single simulation cases: impacts, therefore close approaches, are the objective of analysis and the KS formulation is exactly built to better handle small distances

from the primary. This aspect was highlighted particularly by the much lower time steps taken by the impacting barycenter, more than twenty times lower than the usual Cowell's approach.
Future developments may keep exploring the different branches that were highlighted in this work. Other formulations can be tested, either coordinate-based or element-based, and their performance can be compared with the new benchmark set by the KS formulation that switches between barycentric and planetocentric during flybys. In this regard, the proposed barycentric KS formulation may be studied in the context of the restricted three body problem, seeking for further improvements that can arise from the adaptive time scale. Other development directions may involve the adoption of advanced uncertainty propagation techniques, abandoning the Monte Carlo approach used so far to compute the impact probability in the presented planetary protection example. In fact, despite the improved numerical efficiency brought by the KS coordinates, their principal advantage has not been exploited yet, the almost linear dynamics may analytically improve more efficient methods such as continuum and covariance propagation techniques.

6 ACKNOWLEDGMENTS

The research leading to these results has received funding from the European Research Council (ERC) under the European Union's Horizon2020 research and innovation programme as part of project COMPASS (Grant agreement No 679086), `www.compass.polimi.it`.

7 REFERENCES

REFERENCES

[1] COSPAR, "COSPAR Planetary Protection Policy," Tech. Rep., 2017.

[2] G. Kminek, "ESA planetary protection requirements, Technical Report ESSB-ST-U-001," European Space Agency, Tech. Rep., 2012.

[3] C. Colombo, F. Letizia, and J. Van Der Eynde, "SNAPPshot ESA planetary protection compliance verification software Final report V1.0, Technical Report ESA-IPL-POM-MB-LE-2015-315," University of Southampton, Tech. Rep., 2016.

[4] M. Romano, M. Losacco, C. Colombo, and P. Di Lizia, "Impact probability computation of near-Earth objects using Monte Carlo line sampling and subset simulation," *Celestial Mechanics and Dynamical Astronomy*, vol. 132, no. 8, p. 42, Aug 2020. [Online]. Available: https://doi.org/10.1007/s10569-020-09981-5

[5] M. Romano, "Orbit propagation and uncertainty modelling for planetary protection compliance verification," Ph.D. dissertation, Politecnico di Milano, Supervisors: Colombo, Camilla and Sánchez Pérez, José Manuel, Feb 2020.

[6] C. Colombo, M. Romano, and A. Masat, "SNAPPshot ESA planetary protection compliance verification software Final report V 2.0, Technical Report ESA-IPL-POM-MB-LE-2015-315," Politecnico di Milano, Tech. Rep., 2020.

[7] P. Kustaanheimo, *Spinor Regularization of the Kepler Motion*. Turun Yliopisto, 1964. [Online]. Available: https://books.google.it/books?id=ZhQ9ywAACAAJ

[8] K. F. Sundman, "Mémoire sur le problème des trois corps," *Acta Mathematica*, vol. 36, pp. 105 – 179, 1913. [Online]. Available: https://doi.org/10.1007/BF02422379

[9] P. Kustaanheimo, H. Schinzel, and E. Stiefel, "Perturbation theory of Kepler motion based on spinor regularization," *Journal fur die reine und angewandte Mathematik*, vol. 1965, no. 218, pp. 204–219, 1965. [Online]. Available: https://www.degruyter.com/view/journals/crll/1965/218/article-p204.xml

[10] E. L. Stiefel and G. Scheifele, *Linear and Regular Celestial Mechanics*, ser. Grundlehren der mathematischen Wissenschaften. Springer, Berlin, 1971.

[11] V. R. Bond, "The uniform, regular differential equations of the KS transformed perturbed two-body problem," *Celestial mechanics*, vol. 10, no. 3, pp. 303–318, Sep 1974. [Online]. Available: https://doi.org/10.1007/BF01586860

[12] P. Saha, "Interpreting the kustaanheimo–Stiefel transform in gravitational dynamics," *Monthly Notices of the Royal Astronomical Society*, vol. 400, no. 1, p. 228–231, Nov 2009. [Online]. Available: http://dx.doi.org/10.1111/j.1365-2966.2009.15437.x

[13] S. Breiter and K. Langner, "Kustaanheimo-Stiefel transformation with an arbitrary defining vector," *Celestial Mechanics and Dynamical Astronomy*, vol. 128, no. 2, pp. 323–342, Jun 2017. [Online]. Available: https://doi.org/10.1007/s10569-017-9754-z

[14] J. Waldvogel, "Quaternions and the perturbed Kepler problem," in *Periodic, Quasi-Periodic and Chaotic Motions in Celestial Mechanics: Theory and Applications*, A. Celletti and S. Ferraz-Mello, Eds. Dordrecht: Springer Netherlands, 2006, pp. 201–212.

[15] K. Langner and S. Breiter, "KS variables in rotating reference frame. application to cometary dynamics," *Astrophysics and Space Science*, vol. 357, no. 2, p. 153, May 2015. [Online]. Available: https://doi.org/10.1007/s10509-015-2384-6

[16] J. Roa and J. Peláez, "Orbit propagation in Minkowskian geometry," *Celestial Mechanics and Dynamical Astronomy*, vol. 123, no. 1, pp. 13–43, Sep 2015. [Online]. Available: https://doi.org/10.1007/s10569-015-9627-2

[17] J. Roa, H. Urrutxua, and J. Peláez, "Stability and chaos in Kustaanheimo–Stiefel space induced by the hopf fibration," *Monthly Notices of the Royal Astronomical Society*, vol. 459, no. 3, p. 2444–2454, Apr 2016. [Online]. Available: http://dx.doi.org/10.1093/mnras/stw780

[18] J. Roa and N. J. Kasdin, "Alternative set of nonsingular quaternionic orbital elements," *Journal of Guidance, Control, and Dynamics*, vol. 40, no. 11, pp. 2737–2751, Nov 2017. [Online]. Available: https://doi.org/10.2514/1.G002753

[19] S. Hernandez and M. R. Akella, "Energy preserving low-thrust guidance for orbit transfers in KS variables," *Celestial Mechanics and Dynamical Astronomy*, vol. 125, no. 1, pp. 107–132, May 2016. [Online]. Available: https://doi.org/10.1007/s10569-016-9677-0

[20] R. M. Woollands, J. Read, K. Hernandez, A. Probe, and J. L. Junkins, "Unified Lambert tool for massively parallel applications in space situational awareness," *Journal of the Astronautical Sciences*, vol. 65, no. 1, pp. 29–45, Mar 2018. [Online]. Available: https://doi.org/10.1007/s40295-017-0118-4

[21] H. Sellamuthu and R. K. Sharma, "Orbit theory with lunar perturbation in terms of Kustaanheimo–Stiefel regular elements," *Journal of Guidance, Control, and Dynamics*, vol. 40, no. 5, pp. 1272–1277, 2017. [Online]. Available: https://doi.org/10.2514/1.G002342

[22] ——, "Hybrid orbit propagator for small spacecraft using Kustaanheimo–Stiefel elements," *Journal of Spacecraft and Rockets*, vol. 55, no. 5, pp. 1282–1288, 2018. [Online]. Available: https://doi.org/10.2514/1.A34076

[23] ——, "Regularized luni-solar gravity dynamics on resident space objects," *Astrodynamics*, vol. 5, no. 2, pp. 91–108, Jun 2020. [Online]. Available: https://doi.org/10.1007/s42064-020-0085-6

[24] M. D. Vivarelli, "Geometrical and physical outlook on the cross product of two quaternions," *Celestial mechanics*, vol. 41, no. 1, pp. 359–370, Mar 1987. [Online]. Available: https://doi.org/10.1007/BF01238771

[25] A. Masat, M. Romano, and C. Colombo, "B-plane orbital resonance analysis and applications," Master's thesis, Politecnico di Milano, 2019. [Online]. Available: https://www.diva-portal.org/smash/get/diva2:1440101/FULLTEXT01.pdf

[26] C. M. Will, *The Theoretical Tools of Experimental Gravitation*. California Institute of Technology, Pasadena (CA), USA, 1974.

[27] P. K. Seidelmann, *Explanatory Supplement To The Astronomical Almanac*. University Science Books, 1992.

[28] A. Quarteroni, R. Sacco, and F. Saleri, *Numerical Mathematics Texts in Applied Mathematics*, 2007.

[29] C. H. Acton, "Ancillary data services of NASA's Navigation and Ancillary Information Facility," *Planetary and Space Science*, vol. 44, no. 1, pp. 65–70, Jan 1996. [Online]. Available: https://www.sciencedirect.com/science/article/pii/0032063395001077

[30] E. B. Wilson, "Probable inference, the law of succession, and statistical inference," *Journal of the American Statistical Association*, vol. 22, no. 158, pp. 209–212, 1927. [Online]. Available: http://www.jstor.org/stable/2276774

[31] R. Jehn, "Estimating the impact probability of ariane upper stages," European Space Agency, Tech. Rep. December, 2014.

[32] M. Wallace, "A massively parallel bayesian approach to planetary protection trajectory analysis and design," 2015. [Online]. Available: https://trs.jpl.nasa.gov/handle/2014/45859